

HIGH-EXCITATION EXTRANUCLEAR GAS IN SEYFERT GALAXIES

CHRISTOPHER A. HANIFF

Palomar Observatory, California Institute of Technology

MARTIN J. WARD

Royal Greenwich Observatory, Cambridge

AND

ANDREW S. WILSON

Astronomy Program, University of Maryland

Received 1990 June 4; accepted 1990 August 1

ABSTRACT

We have obtained high-resolution images in the emission lines [O III] $\lambda\lambda 4959, 5007$ and $H\alpha + [N II] \lambda\lambda 6548, 6584$ for three Seyfert galaxies—Mrk 573, NGC 2110, and NGC 5252. In at least Mrk 573 and NGC 2110, the emission line and radio continuum axes are closely related. Maps of the flux ratio [O III] $\lambda 5007 / H\alpha + [N II] \lambda\lambda 6548, 6584$ reveal localized regions of high-excitation gas away from the nucleus of each galaxy. In all cases the off-nucleus excitation is comparable to or higher than that at the nucleus itself, which may reflect increases in the ionization parameter, the presence of optically thin clouds or extra heating sources for the gas. In Mrk 573 and NGC 5252, the distribution of the ionized gas resembles a pair of conical structures, each with its apex at the nucleus, implying preferential escape of ionizing photons in two oppositely directed cones. We speculate on the possible significance that high-excitation gas around Seyfert nuclei is observed preferentially in host galaxies of type S0.

Subject headings: galaxies: individual (NGC 2110, NGC 5252, Markarian 573) — galaxies: interstellar matter — galaxies: nuclei — galaxies: Seyfert

I. INTRODUCTION

The phenomenological division of Seyfert galaxies into types 1 and 2, based on the relative widths of their forbidden and permitted emission lines was proposed by Khachikian and Weedman (1971). This distinction proved useful in early studies which demonstrated the marked overlap of many continuum and emission-line properties of Seyfert 1's and quasars. The Seyfert 2 nuclei were then generally considered to be intrinsically different from the type 1's, although the properties of their narrow-line regions were recognized to be very similar. However, recently much interest has been shown in “unified models” of active galactic nuclei, which seek to explain the lack of broad lines and nonstellar continua in Seyfert 2's as a geometrical effect. In essence, these schemes envisage a torus of material surrounding the active nucleus. In the case of Seyfert 2's, our line of sight to the nucleus intersects the torus, and the nonthermal continuum and broad-line region are both obscured. On the other hand, Seyfert 1's are presumed to be seen directly, so that the torus, although present, does not impede our view of the “central engine.” An important prediction of these models is that any extended gas will be ionized preferentially in directions aligned with the minor axis of the torus.

The observational evidence for this picture is increasingly strong. Emission-line polarization data on the prototypical Seyfert 2 galaxy NGC 1068 have demonstrated the existence of a broad-line region, which is viewed only indirectly via scattering off electrons or dust (Antonucci and Miller 1985). Following on from the NGC 1068 results, a broad-line region has been detected in other Seyfert 2's when observed in polarized light (Miller and Goodrich 1990). Support for anisotropic continuum emission in Seyfert 2's has come from the application of arguments based on the energy requirements of their narrow-

line regions (e.g., Wilson, Baldwin, and Ulvestad 1985, hereafter WBU; Ferland and Osterbrock 1986; Wilson, Ward, and Haniff 1988) and from the morphology of the spatially extended, high-excitation gas (Unger *et al.*, 1987; Haniff, Wilson, and Ward 1988, hereafter HWW). A related approach has involved the study of “excitation maps,” typically the distribution of the flux ratio of [O III] $\lambda 5007$ to $H\alpha$ or $H\beta$. Conical morphologies with the nucleus at the apex have been seen in excitation maps of NGC 1068 (Pogge 1988*a*), NGC 4388 (Corbin, Baldwin, and Wilson 1988; Pogge 1988*b*), NGC 5252 (Tadhunter and Tsvetanov 1989), and NGC 5728 (Schommer *et al.*, 1988; Pogge 1989). All of these observations seem consistent with the possibility that the compact continuum source at the nucleus is hidden from our direct view by an obscuring torus, while the extended line-emitting regions are exposed to the largely unobscured flux of ionizing radiation escaping along the minor axis of the torus.

In this paper we present emission-line excitation maps for the three Seyfert 2 galaxies: Mrk 573, NGC 2110, and NGC 5252. Our observations have been obtained with excellent plate scale ($\leq 0''.2$ per pixel) and seeing ($\approx 1''.2$ FWHM), allowing the distributions of emission-line intensity and excitation to be derived with better spatial resolution than previous studies. The line and continuum images of Mrk 573 have been presented previously in HWW, but that work did not include any excitation maps. Subsequently, Tsvetanov *et al.* (1989) have obtained similar data for Mrk 573. Emission-line images and excitation maps of NGC 5252 have recently been shown in Tadhunter and Tsvetanov (1989). Our data on NGC 5252 are not as deep as their images, and so our discussion is primarily concerned with the excitation gradients in the brighter nebulae close to the nucleus. NGC 2110 was included in the studies by WBU and Pogge (1989), and we compare our results

with theirs in § III. In all three objects we find that discrete regions of high-excitation gas exist away from the nucleus, as defined by the peak of continuum light, and in two cases (Mrk 573 and NGC 5252) there is clear evidence for a conical geometry. In Mrk 573 there is a nuclear region of comparably high excitation to the clouds observed on either side of the nucleus, but in NGC 2110 and NGC 5252, the regions of highest excitation are found several arcsecs away from the nucleus. A Hubble constant of $75 \text{ km s}^{-1} \text{ Mpc}^{-1}$ is used throughout this paper.

II. OBSERVATIONS AND REDUCTION

Narrow-band images of Mrk 573, NGC 2110, and NGC 5252 were obtained during the course of our imaging survey of Seyfert galaxies with "linear" or jetlike radio structure (HWW). The data were obtained at the $f/10$ Cassegrain focus of the University of Hawaii 88" telescope on Mauna Kea using either the IFA/Galileo 500×500 CCD (NGC 2110), which gave an image scale of $0''.14$ per pixel, or the Cambridge GEC 576×385 CCD (Mrk 573, NGC 2110, NGC 5252), which has a pixel size of $0''.2$. The images were taken through narrow-band interference filters, with typical full widths at half-maximum of 100 \AA , isolating the redshifted $\text{H}\alpha + [\text{N II}] \lambda\lambda 6548, 6584$, and $[\text{O III}] \lambda\lambda 4959, 5007$ lines. Since we normalize our excitation maps to give the ratio $[\text{O III}] \lambda 5007 / \text{H}\alpha + [\text{N II}] \lambda\lambda 6548, 6584$, we shall hereafter refer to the latter images simply as $[\text{O III}] \lambda 5007$. Similar line-free continuum integrations were also made at wavelengths as close as possible to the redshifted emission-line frames. Full details of the observations are given in Table 1.

The reduction procedure has been described in detail in our previous paper (HWW), so we shall present only a brief summary here. Having corrected each integration for the bias and dark levels and removed any bad pixels and columns, the images were flat-fielded using dome exposures taken through the appropriate narrow-band filters. For NGC 2110 and Mrk 573, all of the on- and off-line images were then aligned to a

common coordinate grid using field stars as fiducial references, and the corresponding frames coadded. The estimated errors in these transformations, which employed a shift of origin alone, were less than 0.3 pixels ($0''.06$). For NGC 5252, there were no field stars in the CCD frames and so alignment of the images was achieved using the nucleus of the galaxy as the sole reference point. Continuum-free images in the lines of $[\text{O III}] \lambda 5007$ and $\text{H}\alpha + [\text{N II}] \lambda\lambda 6548, 6584$ were then derived by subtracting, once the data had been smoothed to the same effective resolution, suitably scaled versions of the off-line from the on-line images. We estimate that the errors in the scaling factors used were $\sim 10\%$ for NGC 2110 and Mrk 573. The scaling factors for NGC 5252 could not be determined from our data alone due to the absence of field stars, so we have calculated theoretical values based on the measured filter transmission curves and detector efficiency. Our factor for the $[\text{O III}] \lambda 5007$ image agrees well with previous empirical determinations made with the same filter/CCD combination and should be reliable to $\sim 10\%$. The $\text{H}\alpha + [\text{N II}]$ scaling factor is less certain and, based on previous calculations, may be in error by as much as 20%.

To identify the line-emitting regions of highest excitation, we have followed the procedure of Pogge (1988*a, b*) and divided the continuum-free $[\text{O III}] \lambda 5007$ images by the corresponding $\text{H}\alpha + [\text{N II}] \lambda\lambda 6548, 6584$ images. To minimize the possibility of spurious features in the excitation map arising from regions of low signal-to-noise ratio in the line images, the $[\text{O III}] \lambda 5007$ and $\text{H}\alpha + [\text{N II}]$ images of NGC 2110 and NGC 5252 were first smoothed by applying a 5×5 pixel median filter. We have opted to be more conservative than Pogge and only performed the division where both $[\text{O III}] \lambda 5007$ and $\text{H}\alpha + [\text{N II}]$ emission were detected at a level of more than 3σ above the background. In those instances where $\text{H}\alpha$ was detected but $[\text{O III}] \lambda 5007$ was not, the pixels were flagged as low excitation. These regions are not displayed in Figure 1 (Plate 1). Although the observations were not all obtained under photometric conditions, it is still possible to make quantitative estimates of the

TABLE 1
OBSERVING LOG^a

NAME	DATE	NUMBER OF STARS	CCD	SEEING FWHM	EXPOSURE TIME (s)	FILTER WAVELENGTHS (\AA)			
						Band	- 50%	Peak	+ 50%
Mrk 573	1986 Sep 23	2	C	1''.6	2 × 600	On	5080	5120	5170
					2 × 600	Off	5220	5260	5330
	1986 Sep 25	2	C	1''.1	2 × 300	On	6620	6690	6770
					2 × 300	Off	6380	6430	6470
NGC 2110	1987 Feb 21	2	G	1''.2	3 × 600	On	4950	5000	5040
					2 × 600	Off	5100	5150	5190
	1987 Feb 21	2	G	1''.1	2 × 300	On	6580	6650	6700
					1 × 300	Off	6380	6430	6470
NGC 2110	1988 Nov 12	2	C	1''.2	2 × 600	On	5040	5075	5110
					2 × 600	Off	5150	5200	5250
NGC 5252	1988 Jan 21	0	C	1''.2	1 × 300	On	5080	5120	5170
					1 × 300	Off	5220	5260	5330
	1988 Jan 21	0	C	1''.2	1 × 300	On	6620	6700	6770
					1 × 300	Off	6180	6250	6320

^a The columns of this table give (from left to right): name of galaxy, UT date of observation, number of stars used to align the on- and off-band images, the CCD camera used (G = IFA Galileo, C = Cambridge GEC), the seeing, number of images and exposure times used and the filter wavelengths (at peak and at 50% of the peak transmission). For NGC 5252, the seeing was estimated from exposures taken immediately before these observations. The 1987 seeing measurements for NGC 2110 refer to the FWHM along the minor axes of the trailed images (see § II).

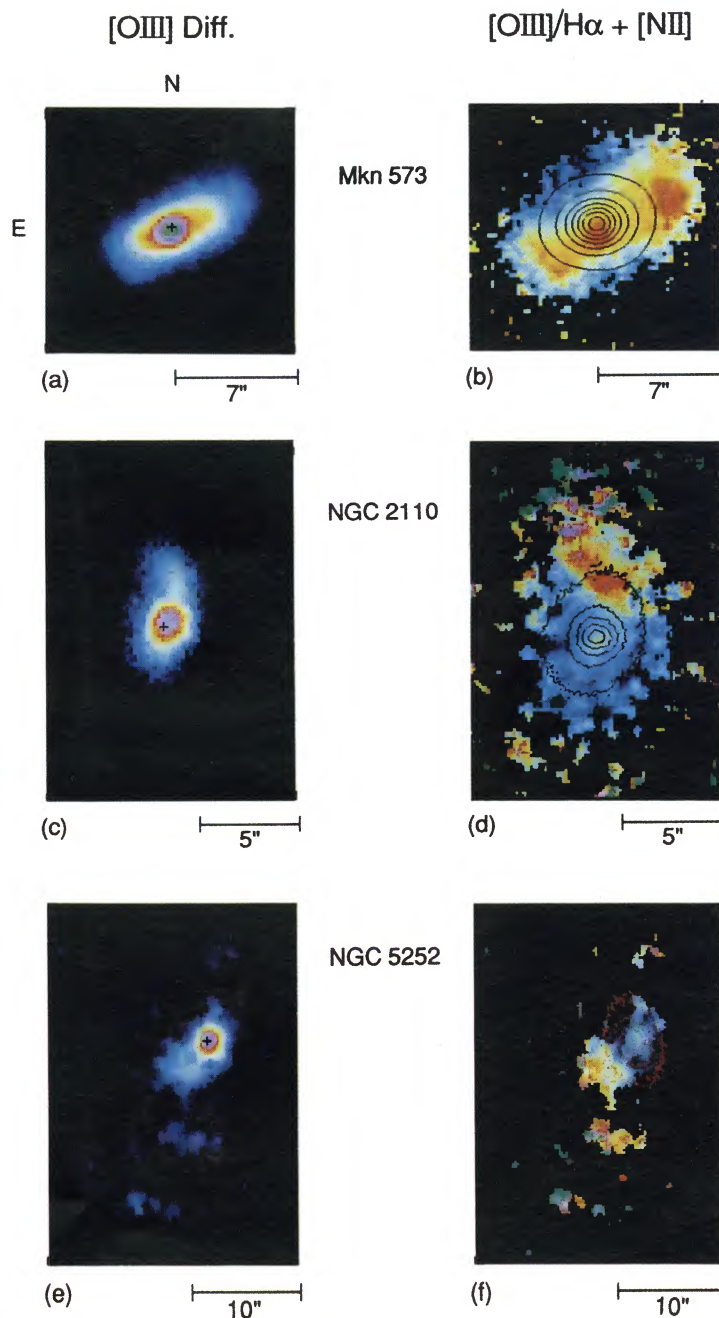


FIG. 1.—(a) Mrk 573: [O III] $\lambda\lambda 4959, 5007$ continuum subtracted image, 0.2 arcsec per pixel. The black cross marks the peak of the red narrow-band continuum image (see Table 1). The color representation, in terms of counts above the background is as follows: dark blue ~ 80 , pale blue ~ 210 , white ~ 300 , yellow ~ 520 , red ~ 725 , pink ~ 920 , and green ~ 1250 . (b) Mrk 573: Ratio map, [O III] $\lambda 5007/H\alpha + [N II] \lambda\lambda 6548, 6584$, 0.2 arcsec per pixel. The black contours superposed are those of the red continuum image. The \mathcal{R} values are color coded as follows: dark blue ~ 0.6 , pale blue ~ 0.8 , white ~ 1.6 , yellow ~ 1.9 , and dark orange ~ 2.4 . (c) NGC 2110: [O III] $\lambda\lambda 4959, 5007$ continuum subtracted image, 0.2 arcsec per pixel. The black cross marks the peak of the green narrow-band continuum image. The color representation, in terms of counts above the background is as follows: dark blue ~ 40 , pale blue ~ 65 , white ~ 110 , yellow ~ 160 , red ~ 200 , and pink ~ 270 . (d) NGC 2110: [O III] $\lambda 5007/H\alpha + [N II] \lambda\lambda 6548, 6584$, 0.14 arcsec per pixel. The black contours superposed are those of the red continuum image. Note that the [O III] $\lambda 5007$ image used to produce this map is somewhat less deep than that shown in Fig. 1c (see Table 1). The \mathcal{R} values are color coded as follows: dark blue ~ 0.15 , pale blue ~ 0.27 , white ~ 0.40 , yellow ~ 0.50 , orange ~ 0.70 , and pink ~ 0.85 . Green pixels represent those regions where only [O III] emission was detected. (e) NGC 5252: [O III] $\lambda\lambda 4959, 5007$ continuum subtracted image, 0.2 arcsec per pixel. The black cross marks the peak of the red narrow-band continuum image. The color representation, in terms of counts above the background is as follows: dark blue ~ 10 , pale blue ~ 20 , white ~ 30 , yellow ~ 50 , red ~ 65 , and pink ~ 90 . (f) NGC 5252: Ratio map, [O III] $\lambda 5007/H\alpha + [N II] \lambda\lambda 6548, 6584$, 0.2 arcsec per pixel. The red contours superposed are those of the red continuum image. The \mathcal{R} values are color coded as follows: dark blue ~ 0.10 , pale blue ~ 0.15 , white ~ 0.25 , yellow ~ 0.30 , orange ~ 0.40 , and pink ~ 0.50 . Green pixels represent those regions where only [O III] emission was detected.

HANIFF, WARD, AND WILSON (see 368, 168)

flux ratio (\mathcal{R}) of $[\text{O III}] \lambda 5007/\text{H}\alpha + [\text{N II}]$ by comparing our line images with the nuclear spectrophotometry of Koski (1978), Shuder (1980), and Ulvestad and Wilson (1983a). These authors present line flux measurements made through apertures of typically several arcsecs centered on the nuclei of NGC 2110 and Mrk 573. We have used their measurements to scale our flux maps, so that when these maps are summed over their aperture sizes, the resulting values of \mathcal{R} agree with their published values. At present there are no published emission-line ratios for NGC 5252, so Figure 1f shows the relative, rather than absolute, distribution of \mathcal{R} over the galaxy.

The $[\text{O III}] \lambda 5007$ difference map of NGC 2110 shown in Figure 1c was derived from data taken during good observing conditions in 1988 November. However, the corresponding excitation map (Fig. 1d) was prepared from long-exposure integrations, taken in 1987 February, which were subject to significant wind-shake, and hence the field star images are elongated along P.A. = 90° , with axial ratios of between 1.4 and 1.6. This introduces some degree of uncertainty when attempting to interpret the detailed morphology of this excitation map. Nevertheless, based on data taken on other nights during this observing run and on the large extent of the features that we have identified, we are confident that our conclusions concerning the overall extent and spatial distribution of the high-excitation gas remain valid. In order to quantify the effects of inaccurate continuum subtraction during the preparation of the individual $[\text{O III}]$ and $\text{H}\alpha$ line maps, and the possibility of incorrect alignment of the maps prior to their division, we repeated our analysis after introducing deliberate errors in both the continuum scaling factors ($\pm 10\%$) and during the frame registration (± 1 pixel). In all cases, apart from modifying the fine structure on a pixel-to-pixel scale, there was little variation in the overall distribution of the high-excitation gas, and the structures reported in § III could always be clearly discerned.

III. MAPS OF EMISSION LINE FLUXES AND RATIOS

The principal new results of the present paper concern the distributions of the flux ratio $\mathcal{R} = [\text{O III}] \lambda 5007/\text{H}\alpha + [\text{N II}] \lambda\lambda 6548, 6584$ over the spatially resolved regions of Mrk 573, NGC 2110, and NGC 5252. The most interesting aspects of these distributions are the high values of \mathcal{R} , the conical morphologies of the high-excitation gas in two of the galaxies, and the relation of the distributions of \mathcal{R} to the radio structures. In the following discussion, all the values of \mathcal{R} quoted represent local averages over circular regions of radius 2 pixels.

Our $[\text{O III}] \lambda 5007$ and $\text{H}\alpha + [\text{N II}] \lambda\lambda 6548, 6584$ images of Mrk 573 have been presented in HWW. The $[\text{O III}] \lambda 5007$ image (Fig. 1a) reveals an elongated emission-line nebulosity of $\sim 13''$ (4.4 kpc) which is closely aligned with the radio axis. Our data permit the evaluation of \mathcal{R} over a rectangular area centered on the continuum peak, in which a “bow-tie” shaped region of higher excitation gas is clearly visible. This comprises a peak ($\mathcal{R} = 2.4$) offset some $0.8''$ to the southwest of the continuum peak, together with two fans of high-excitation gas extending toward the northwest and southeast (Fig. 1b). This result strongly suggests the presence of two oppositely directed cones of ionizing radiation in Mrk 573, each with apparent full apex angle $\sim 45^\circ$. The elongated distribution of \mathcal{R} extends $\sim 10''$ (3.4 kpc) in P.A. = $120^\circ \pm 4^\circ$, the same direction as the major axes of the $[\text{O III}] \lambda 5007$ (P.A. = 116°) and radio continuum (P.A. 122°) isophotes (HWW). Away from the central knot of high-excitation gas the flux ratio \mathcal{R} initially decreases, taking values of 1.8 and 1.9 to the NW and SE, respectively.

However, at the ends of the bow-tie feature, spatially resolved peaks in \mathcal{R} are found, with $\mathcal{R} \simeq 2.5$ (NW peak) and $\mathcal{R} \simeq 2.1$ (SE peak). The two peaks lie $\simeq 4.4''$ (= 1.5 kpc, NW peak) and $\simeq 3.1''$ (= 1.0 kpc, SE peak) from the nucleus, as defined by the peak of the continuum light (Fig. 1b). These distances are considerably larger than the displacements of the two outer radio components from the nucleus ($1.5'' = 500$ pc, NW lobe; $1.4'' = 470$ pc SE lobe, see HWW and Ulvestad and Wilson 1984). These differences of location between the radio lobes and the peaks in \mathcal{R} persist even when the radio maps are smoothed to the resolution of the optical images (cf., Fig. 7 of HWW). A region of lower excitation gas surrounds the high-excitation bow-tie (Fig. 1b).

For NGC 2110 we show both the continuum subtracted $[\text{O III}] \lambda 5007$ image and the excitation map (Figs. 1c and 1d). Maps of the $[\text{O III}]$ morphology have been published by WBU and Pogge (1989), and our map is consistent with these previous data. The $[\text{O III}]$ image (Fig. 1c) shows a resolved nuclear core source, elongated in position angle $\sim 162^\circ$, which is quite similar to the axis (0°) of the jet-like radio source close to the nucleus (Ulvestad and Wilson 1983b). The $[\text{O III}]$ emission decreases much more slowly to the north of the nucleus than to the south, unlike the more symmetrically disposed radio emission. The northern “plume” curves toward the northeast and is directed in position angle $\sim 37^\circ$ at $4''$ from the nucleus. The bending of the $[\text{O III}]$ morphology north of the nucleus is in the same sense as that of the radio continuum structure (Ulvestad and Wilson 1983b). Consideration of the excitation map reveals that the distribution of \mathcal{R} is also asymmetric about the nucleus. At the nucleus itself, defined as the continuum peak (see Fig. 1d), $\mathcal{R} = 0.43$. To the south both the brightness of $[\text{O III}] \lambda 5007$ and \mathcal{R} decrease rapidly over a scale of $\sim 2''$ (290 pc), and at this distance from the nucleus \mathcal{R} is ~ 0.2 . To the north \mathcal{R} reaches a peak value of 0.8 some $3''$ – $4''$ (430–580 pc) from the nucleus, with an average value of 0.7 over the prominent, elongated region of high-excitation gas (see Fig. 1d). In contrast to the interpretation of Pogge (1989), we argue that the areas of highest excitation do not define a clear cone-like morphology, but rather highlight the region where the $[\text{O III}]$ plume bends toward P.A. = 37° . As for Mrk 573, the spatial displacement from the nucleus of the off-nuclear peak in \mathcal{R} for NGC 2110 ($3''$ – $4''$) is larger than the displacement from the nucleus of the radio component on the same side ($1.5''$ – $2.0''$). This difference is not a consequence of the better resolution of the 6 cm radio map since a comparison of the \mathcal{R} distribution with the 20 cm radio map of Ulvestad and Wilson (1983b), which has similar spatial resolution to the optical data, leads to the same conclusion.

Our continuum-subtracted $[\text{O III}] \lambda 5007$ image of NGC 5252 (Fig. 1e) is less sensitive than that presented by Tadhunter and Tsvetanov (1989), and consequently less detail is seen in the faint outer structure. However, the smaller pixels of our image give a better representation of the compact regions close to the nucleus. The $[\text{O III}]$ emission near the nucleus comprises a resolved core and two broad plumes, one extending toward the NW in P.A. = -35° for $\sim 2''$, and the other stretching toward the SE in P.A. = 135° for $\sim 4.5''$. In addition, the brighter limbs of the arclike structures found by Tadhunter and Tsvetanov (1989) are visible some $9''$ to the NW and $9''$ and $15''$ to the SE of the nucleus. For NGC 5252 the distribution of \mathcal{R} (Fig. 1f) shows that the nucleus and the regions within $2''$ of it are of substantially lower excitation than the rest of the nebulosity. The extranuclear plume centered some $3''$ to the SE of the nucleus is of high excitation, with an average value of \mathcal{R}

some two times greater than that measured at the location of the peak of the continuum emission. Three other blobs of high-excitation gas are visible—two of them equispaced on either side of the nucleus at a distance of 9" along P.A. = 173°, and the other situated 15" from the nucleus along P.A. = 164°.

IV. DISCUSSION

a) Galaxy and Emission-Line Morphologies

We begin by discussing a point that may be of general relevance to the observed morphology of the extended high-ionization gas in active galaxies. All three of the galaxies discussed here are of type S0. This contrasts with the fact that many Seyfert 2 nuclei are found in spirals. Although a larger sample is needed for a definitive conclusion to be drawn, our data suggest that the most pronounced examples of the off-nuclear, high-excitation gas phenomenon may be found in S0 host galaxies. If this is the case, the following effects provide a natural explanation. It is well known that the rate of massive star formation in S0 galaxies is lower than in spirals. In this sense, the nuclear environment in active S0's may be expected to be simpler, with the nuclear source dominating the photoionization of the ambient gas. Although nuclear photoionization certainly occurs near the Seyfert nuclei of spiral host galaxies, there will often be an additional component present, namely an ionizing continuum from hot young stars. The excitation of this component will be lower than that for the gas ionized by radiation from the nucleus, thus diluting the regions of highest excitation. Conversely, the contrast of the high excitation gas in S0's will be greatest, making such galaxies the best candidates for the detection of linear and bipolar emission-line morphologies. Furthermore, if the interstellar density is lower in S0's than in spirals, a nuclear ultraviolet source of given luminosity will be able to photoionize the gas to a greater distance in the former galaxies, producing more prominent high-excitation extranuclear nebulosities. Lastly, as emphasized by Meurs (1989), any interstellar gas in S0 galaxies may have been accreted from outside and could be distributed in a "warped" configuration, covering a range of different planes. The chances of intersecting a radiation cone would then be enhanced in comparison with the situation in a normal spiral with a single disk of such gas. Our scenario suggests a possible continuity from the small, high-excitation nebulosities in spiral Seyferts, through nebulosities of intermediate scale in S0's, to the very large nebulosities (up to 100 kpc and beyond) around some radio galaxies (e.g., Fosbury 1989).

Of the three galaxies investigated, both Mrk 573 and NGC 5252 show clear conical morphologies for the ionized gas, while the gas in NGC 2110 is distributed asymmetrically, being much brighter, and of higher excitation, to the north of the nucleus than to the south. We believe, nevertheless, that our results are not inconsistent with the presence of cones in all three objects. Rather special conditions are necessary for a simple bidirectional, symmetric, conical structure to be seen. These conditions are: (1) the line of sight from the observer to the nucleus should not lie within a cone; hence for wide cones, the cone's axis must be close to the plane of the sky, (2) gas should be distributed throughout the entire solid angle subtended by the radiation cone and also at a range of distances from the nucleus, so that the observed emission lines effectively trace the distribution of ionizing photons, not that of the gas, and (3) obscuration by dust should not hide a significant fraction of one or both cones. If any one of these conditions is not satisfied, the conical structures may be hard to recognize.

b) Spatial Gradients in the Gaseous Excitation

Before attempting to interpret the maps presented in Figures 1a–1f, it is important to identify any mechanisms that might alter the ratio $\mathcal{R} = [\text{O III}] \lambda 5007/\text{H}\alpha + [\text{N II}] \lambda\lambda 6548, 6584$, but which are not related to the intrinsic excitation of the gas. Spatial gradients in the value of \mathcal{R} can result from changes in any one of, or a combination of, the following parameters.

1. The excitation, $[\text{O III}] \lambda 5007/\text{H}\alpha$.
2. The ratio $[\text{O III}] \lambda 5007/[\text{N II}] \lambda\lambda 6548, 6584$.
3. The reddening.

Possibility (3) can be investigated by means of our continuum images, the wavelengths of which are close to the (redshifted) $[\text{O III}] \lambda 5007$ and $\text{H}\alpha$ lines, respectively. By taking the ratio of these images it is possible to construct crude color maps of the nuclear regions of these galaxies. In Mrk 573 the continuum ratio map shows a region of relatively redder color $\sim 1''$ north of the core (consistent with higher reddening) and a general trend for a bluer color further north and also away from the nucleus to the SE and NW, along the length of the high-excitation bow-tie, and towards the south. There are no changes in the continuum ratio that might explain the localized features seen in the $[\text{O III}] \lambda 5007/\text{H}\alpha + [\text{N II}]$ ratio image. For NGC 2110 the reddest colors are found on the nucleus and around that part of the northern lobe of highest excitation gas closest to the nucleus. So in this case, if these color gradients represent changes in reddening, correction for reddening can only increase the off-nucleus intrinsic $[\text{O III}] \lambda 5007$ to $\text{H}\alpha + [\text{N II}]$ ratio. Unfortunately the continuum images of NGC 5252 are not deep enough to derive color gradient information. In Mrk 573 and NGC 2110, there are no unambiguous instances where regions of low \mathcal{R} coincide with regions of high reddening, as deduced from the green-to-red continuum ratio maps. Thus we conclude that the observed variations in the value of \mathcal{R} are unlikely to be a consequence of spatial variations in the reddening.

The contribution of variations in the $[\text{O III}] \lambda 5007/[\text{N II}] \lambda\lambda 6548, 6584$ ratio (possibility 2) can be estimated in NGC 2110 from the long-slit spectrophotometry of WBU. Their Figure 7b shows that both $[\text{O III}] \lambda 5007/\text{H}\beta$ and $[\text{N II}] \lambda\lambda 6584/\text{H}\alpha$ increase from south to north over the nebulosity, with the increase between the nucleus and 5" N of it being particularly pronounced for both ratios. Thus, the effect of the inclusion of $[\text{N II}] \lambda\lambda 6548, 6584$ within the passband of the $\text{H}\alpha$ filter is to reduce the gradient in excitation ratio, \mathcal{R} , below that which would be obtained if the $\text{H}\alpha$ line alone were included. This conclusion is strongly supported by other results of WBU, who also found that the $[\text{O III}] \lambda 5007/\text{H}\beta$ ratio varies by at least a factor of 6 over the nebulosity in NGC 2110, with the most highly ionized gas being located to the north of the nucleus.

For Mrk 573 and NGC 5252, the spatial distributions of $[\text{O III}] \lambda 5007/\text{H}\beta$ and $[\text{N II}] \lambda\lambda 6584/\text{H}\alpha$ have not been measured, so there remains some ambiguity in the interpretation of the observed variations in \mathcal{R} for these galaxies. Nevertheless, for the purposes of the following discussion, we shall assume that the variations in \mathcal{R} for Mrk 573 and NGC 5252 are dominated by an intrinsic variation in the excitation of the line-emitting gas, as is the case in NGC 2110.

c) The Nature of High-Excitation Extranuclear Gas

In discussing the nature of the highly excited gas outside the nuclei of Mrk 573, NGC 2110 and NGC 5252, we shall initially assume that this gas is photoionized by a compact nuclear

source. This assumption is reasonable since the nuclear emission-line ratios in Seyfert galaxies imply photoionization by a hard ultraviolet and X-ray continuum source. Measurements of the line ratios in the off-nuclear gas are more limited, but in the case of Seyferts with emission-line gas associated with linear radio sources, the line ratios fall in or near the "power-law" ionized regions of BPT (Baldwin, Phillips, and Terlevich 1981; Veilleux and Osterbrock 1987) diagrams (e.g., Balick and Heckman 1979; WBU; Baldwin, Wilson, and Whittle 1987; Whittle *et al.* 1988). In some cases, there is evidence that the gas is illuminated by UV radiation which is more intense than that emitted toward the Earth (Wilson, Ward, and Haniff 1988). For the moment, we do not consider other contributions, such as local sources of ionizing photons and shock waves, but shall return to these possibilities later. Because the regions of highest excitation are further away from the nucleus than are the radio lobes we shall also ignore contributions to the heating and ionization of the gas by relativistic particles.

Returning to the unified scheme for Seyferts, it is important to note that the presence of a collimating torus does not provide a complete explanation for localized regions of high-excitation, off-nuclear gas along the axis of the torus. Other effects are also required, such as a local reduction in electron density, n_e . Although a more complete study of the line ratios is desirable, the localized peaks in the ratio \mathcal{R} suggest an increased ionization parameter $U = Q(H)/4\pi n_e r^2 c$, where $Q(H)$ is the number of ionizing photons emitted by the source, and r the distance between the central ionizing source and the gas. Discrete peaks in U then suggest that locally n_e is declining with radius faster than r^{-2} . A decline in density is qualitatively consistent with the rapid drop off in the [O III] $\lambda 5007$ and $H\alpha + [N II] \lambda\lambda 6548, 6584$ line brightnesses at the locations of the peaks in \mathcal{R} in all three galaxies. It is possible that these rapid decreases in line brightness are simply associated with the edge of the gaseous disk in the host galaxy. A more complicated scenario would envisage the radio components driving radiative bow shocks into a uniform ambient medium (cf., Pedlar, Dyson, and Unger 1985; Wilson and Ulvestad 1987). The radio clouds would then be surrounded by dense gas, but upstream in front of the bow shock, the density of the gas would take its lower ambient value. If the ionizing radiation were also beamed along the radio axis, the result would be a localized peak in U just ahead of the bow shock. Still further upstream of the shock, U would decline because of its r^{-2} dependence in a uniform medium. The alignment of the highest excitation gas with the radio axis in Mrk 573 is, therefore, consistent with the ionizing continuum being directed along the radio axis, while in NGC 2110 the ionizing continuum must have an opening angle that includes the S-shaped, jetlike, radio source.

An increase in the [O III] $\lambda 5007/H\alpha$ ratio could also imply the presence of optically thin clouds (cf., Viegas-Aldrovandi 1988). In most models of the emission-line regions in Seyferts, the clouds are optically thick (radiation bounded) and contain stratified zones, with the most highly ionized gas on the side of the cloud facing the ionizing source. In the interior, an extended, partially neutral zone is heated by the penetrating high-energy photons (e.g., Ferland and Shields 1985). If such a cloud is truncated and becomes optically thin (matter bounded), the O^{++} zone could be unaffected, but the region contributing to the recombination lines is reduced in size, so the ratio [O III] $\lambda 5007/H\alpha$ would increase.

Above we have assumed that the ionizing photons originate in the Seyfert nucleus. However, there are various other possible sources of *in situ* photoionization. These include: stellar radiation, extended synchrotron emission, and thermal bremsstrahlung from hot gas in the vicinity of the radio lobes. High flux ratios [O III] $\lambda 5007/H\alpha$ can result from low metallicity H II regions ionized by hot stars (e.g., Dopita and Evans 1986). Ionization by hot stars is, however, unlikely to be responsible for the high excitations observed, since the nuclear continuum spectra of Mrk 573 and NGC 2110 are known to be dominated by old stellar populations (Koski 1978; WBU). While the stellar population could be different off the nucleus, there is no evidence in the continuum images for the expected clumps of blue stars at the locations of the high-excitation gas. Ultraviolet synchrotron radiation from the extended radio components is another possibility. Although the emission-line and radio morphologies are related, there is not the *detailed* correspondence one would expect if this were the primary source of extranuclear ionization. Also, extrapolation of the radio spectra yields ionizing photon luminosities orders of magnitude below those required to ionize the extranuclear gas. Little is known about the presence of hot gas in the circumnuclear environment of Seyfert galaxies. Elvis *et al.* (1990) have recently reported the detection of extended soft X-ray emission in three Seyfert galaxies. Separation of the nuclear and extranuclear X-ray components on the scale of the extended gas in Mrk 573 and NGC 2110, will require much greater sensitivity and resolution than previously available, and will have to await future X-ray missions such as *AXAF*.

A quite different mechanism is collisional ionization in shock waves. Even if shocks are not an important source of ionization (as indicated by the line ratios), they could contribute to the excitation by providing an extra source of heating. Shocks driven ahead of the radio lobes into thermal gas already photoionized by the nuclear radiation field can lead to anomalous line ratios (see Viegas-Aldrovandi and Contini 1989). Well ahead of the shock, and also in the recombination zone behind it, heating and ionization are probably dominated by photons from the nuclear source. However, between these two regions, the gas is heated by the shock to temperatures in excess of those typical of photoionized gases, and anomalous [O III] $\lambda 5007/H\alpha$ ratios would result. It is interesting to note that Tadhunter, Robinson, and Morganti (1989) have recently found that, for a number of extended emission-line regions, the temperatures of the line-emitting gas (as derived from the observed line ratio [O III] $\lambda 4363/[O III] \lambda\lambda 4959, 5007$) are considerably higher than those expected on the basis of photoionization models. Their data refer primarily to radio galaxies, but also include NGC 5252. They conclude that the effect results either from additional heating sources (such as shocks) in the photoionized gas or from subsolar abundances. Further measurements of the [O III] $\lambda 4363$ line would be valuable for checking whether this anomaly is also present in the extended emission-line regions of Seyfert galaxies.

V. CONCLUSIONS

The main results of this study are the following:

1. Line ratio maps, in conjunction with long-slit spectroscopy, provide a powerful means by which to study the morphology and excitation of the extended emission-line gas around active nuclei. In particular, they reveal structures that can remain hidden in images taken in the light of a single

emission line, even if it traces a relatively high-excitation species such as O^{++} .

2. Regions of highly excited gas are observed away from the optical nucleus in a number of Seyfert galaxies. In some cases, the excitation ratio $[O\ III] \lambda 5007/H\alpha + [N\ II] \lambda \lambda 6548, 6584$ is higher at these off-nuclear locations than at the nucleus itself.

3. Conical shapes (with apices at the nucleus) of high-excitation gas have now been found in five Seyfert 2 galaxies—NGC 1068, NGC 4388, NGC 5252, NGC 5728, and Mrk 573. These morphologies are consistent with collimation of the ionizing photons by an obscuring torus or by a radiation pressure supported torus (Acosta Pulido *et al.*, 1990). Such morphologies are, however, not always found. In NGC 2110, for example, the distribution of high-excitation gas is highly asymmetric. While this could reflect an intrinsically different geometry or origin for the ionizing radiation, such asymmetries are, however, entirely consistent with the presence of conical emission-line regions suffering differential extinction. Indeed, it is to be expected that the clearest examples of biconical emission-line regions will only be seen when viewed from a favorable orientation, when gas fills most of the solid angle of the ionizing cones, and when strong and differential obscuration is absent. These effects can mask the presence of conical emission-line morphologies even when the ionizing radiation does escape from the nucleus along two oppositely directed cones.

4. The cause of these localized off-nuclear regions of high-excitation gas is not known. They may result from a local increase in the ionization parameter, the presence of optically

thin clouds, or extra heating sources for the gas. In principle, line ratio diagnostics yielding information on density and temperature gradients in the extended line-emitting gas could provide the answer. These observations are feasible but difficult, requiring a combined effort using large ground-based optical telescopes, and the high spatial resolution of the HST.

5. It seems that the best examples of this kind of high-excitation extranuclear emission-line gas in Seyfert galaxies are found around nuclei residing in type S0 host galaxies. This could result from a number of factors—the absence of H II regions, a low interstellar density and non-coplanar gas disks—all of which favor the identification of extended ionized gas in S0's compared with late-type spirals. The high-excitation nebulosities in S0's with active nuclei may be intermediate in size between the compact (\leq kpc) nebulosities seen around the nuclei of spiral Seyferts and the very large (hundreds of kpc) nebulosities found in some radio galaxies. Investigation of a larger sample of AGN residing in S0 galaxies is, however, required to test these suggestions.

We thank the Institute for Astronomy at the University of Hawaii for awarding us telescope time, and for technical support during the observations. Financial support is acknowledged from Christ's College Cambridge (C. A. H.) in the form of a Research fellowship. M. J. W. acknowledges the tenure of an SERC advanced fellowship during the majority of this work. This research was supported by grants from the National Science Foundation (AST-8719207) and NASA (NAG5-1079 and NAG8-529) to the University of Maryland.

REFERENCES

- Acosta Pulido, J., Calvani, M., Pérez-Fournon, I., and Wilson, A. S. 1990, *Ap. J.*, **365**, 119.
- Antonucci, R. R. J., and Miller, J. S. 1985, *Ap. J.*, **297**, 621.
- Baldwin, J. A., Phillips, M. M., and Terlevich, R. 1981, *Pub. A.S.P.*, **93**, 5.
- Baldwin, J. A., Wilson, A. S., and Whittle, D. M. 1987, *Ap. J.*, **319**, 84.
- Balick, B., and Heckman, T. M. 1979, *A.J.*, **84**, 302.
- Corbin, M. A., Baldwin, J. A., and Wilson, A. S. 1988, *Ap. J.*, **334**, 584.
- Dopita, M. A., and Evans, I. N. 1986, *Ap. J.*, **307**, 431.
- Elvis, M., Fasnacht, C., Wilson, A. S., and Briel, U. 1990, *Ap. J.*, **361**, 459.
- Ferland, G. J., and Osterbrock, D. E. 1986, *Ap. J.*, **300**, 658.
- Ferland, G. J., and Shields, G. A. 1985, in *Astrophysics of Active Galaxies and Quasi-Stellar Objects*, ed. J. S. Miller (Mill Valley, CA: University Science Books), p. 157.
- Fosbury, R. A. E. 1989, in *Extranuclear Activity in Galaxies*, ed. E. J. A. Meurs and R. A. E. Fosbury, (Garching: ESO), p. 169.
- Haniff, C. A., Wilson, A. S., and Ward, M. J. 1988, *Ap. J.*, **334**, 104 (HWW).
- Khachikian, E. Ye., and Weedman, D. W. 1971, *Astrofizika*, **7**, 389.
- Koski, A. T. 1978, *Ap. J.*, **223**, 56.
- Meurs, E. J. A. 1989, in *Extranuclear Activity in Galaxies*, ed. E. J. A. Meurs and R. A. E. Fosbury, (Garching: ESO), p. 405.
- Miller, J. S., and Goodrich, R. W. 1990, *Ap. J.*, **355**, 456.
- Pedlar, A., Dyson, J. E., and Unger, S. W. 1985, *M.N.R.A.S.*, **214**, 463.
- Pogge, R. W. 1988a, *Ap. J.*, **328**, 519.
- . 1988b, *Ap. J.*, **332**, 702.
- Pogge, R. W. 1989, *Ap. J.*, **345**, 730.
- Schommer, R. A., Caldwell, N., Wilson, A. S., Baldwin, J. A., Phillips, M. M., Williams, T. B., and Turtle, A. J. 1988, *Ap. J.*, **324**, 154.
- Shuder, J. M. 1980, *Ap. J.*, **240**, 32.
- Tadhunter, C., Robinson, A., and Morganti, R. 1989, in *Extranuclear Activity in Galaxies*, ed. E. J. A. Meurs and R. A. E. Fosbury, (Garching: ESO), p. 293.
- Tadhunter, C., and Tsvetanov, Z. 1989, *Nature*, **341**, 422.
- Tsvetanov, Z., Tadhunter, C., Pérez, E., and González-Delgado, R. 1989, in *Extranuclear Activity in Galaxies*, ed. E. J. A. Meurs and R. A. E. Fosbury (Garching: ESO), p. 19.
- Ulvestad, J. S., and Wilson, A. S. 1983a, *A.J.*, **88**, 253.
- . 1983b, *Ap. J. (Letters)*, **264**, L7.
- . 1984, *Ap. J.*, **278**, 544.
- Unger, S. W., Pedlar, A., Axon, D. J., Whittle, M., Meurs, E. J. A., and Ward, M. J. 1987, *M.N.R.A.S.*, **228**, 671.
- Veilleux, S., and Osterbrock, D. E. 1987, *Ap. J. Suppl.*, **63**, 295.
- Viegas-Aldrovandi, S. M. 1988, *Ap. J. (Letters)*, **330**, L9.
- Viegas-Aldrovandi, S. M., and Contini, M. 1989, *Ap. J.*, **339**, 689.
- Whittle, D. M., Pedlar, A., Meurs, E. J. A., Unger, S. W., Axon, D. J., and Ward, M. J. 1988, *Ap. J.*, **326**, 125.
- Wilson, A. S., Baldwin, J. A., and Ulvestad, J. S. 1985, *Ap. J.*, **291**, 627 (WBU).
- Wilson, A. S., and Ulvestad, J. S. 1987, *Ap. J.*, **319**, 105.
- Wilson, A. S., Ward, M. J., and Haniff, C. A. 1988, *Ap. J.*, **334**, 121.

CHRISTOPHER A. HANIFF: Palomar Observatory, California Institute of Technology, Pasadena, CA 91125

MARTIN J. WARD: Royal Greenwich Observatory, Madingley Road, Cambridge, CB3 0EZ, England, UK

ANDREW S. WILSON: Astronomy Program, University of Maryland, College Park, MD 20742